fluids

MDPI

Article

Time-Dependent Motion of a Floating Circular Elastic Plate

Michael H. Meylan

School of Mathematical and Physical Sciences, The University of Newcastle, Callaghan, NSW 2308, Australia; mike.meylan@newcastle.edu.au

Abstract: The motion of a circular elastic plate floating on the surface is investigated in the time-domain. The solution is found from the single frequency solutions, and the method to solve for the circular plate is given using the eigenfunction matching method. Simple plane incident waves with a Gaussian profile in wavenumber space are considered, and a more complex focused wave group is considered. Results are given for a range of plate and incident wave parameters. Code is provided to show how to simulate the complex motion.

Keywords: hydroelasticity; floating plate; linear water waves

Citation: Meylan, M.H. Time-Dependent Motion of a Floating Circular Elastic Plate. *Fluids* **2021**, *6*, 29. https://doi.org/10.3390/fluids6010029

Received: 16 December 2020
Accepted: 6 January 2021
Published: 8 January 2021

1. Introduction

The single frequency solution for the linear water wave problem is extensively used to model the hydroelastic response of very large floating structures, container ships, or an ice floe [1–4]. The simplest example problem in hydroelasticity is the floating elastic plate, which has been the subject of extensive research. Many different methods of solution have been developed, including Green function methods [5,6], eigenfunction matching [7–9], multi-mode methods [10] and the Wiener–Hopf method [11,12].

The problem becomes more complicated if we consider the time-dependent problem. If the floating plate is assumed to be of infinite extent, the problem becomes simpler and a spatial Fourier transform gives the solution [13–19]. The forced vibration of a finite floating elastic plate was solved by [20] using a variational formulation and the Rayleigh–Ritz method. The problem was analyzed in shallow water by [21–23] and in finite depth by [24]. The solution for incident waves in two-dimensions was given in finite depth by [25–27] and in shallow water in two by [21,22] and three–dimensions by [23]. A comparison for the time–dependent motion in two-dimensions for an initial condition was given in [28]. The solution for finite water depth in three–dimensions was found by [29–32] and was experimentally investigated by [33]. The solution due to a transient incident wave forcing was given in [34]. Recently, there has been extensive work on nonlinear simulations using computational fluid dynamics to investigate nonlinear phenomena [35–38]. However, even for the case of high amplitude waves, the linear wave problem remains valid for a floating plate [39], and this model continues to the basis of offshore engineering and scattering by an ice floe.

The eigenfunction matching method has been applied to many floating elastic plate problems. It has proved to give the most uncomplicated solutions, provided that the geometry is sufficiently simple that it can be applied. The solution method was first described in [7] and this is where the solution of the special dispersion equation for a floating elastic plate was introduced. This method was extended to circular [9], multiple [40–42], and submerged elastic plates [43,44].

We present here a solution to the time-dependent problem of a floating circular plate subject to incident wave forcing. In part, the purpose of this work is to show how simply the complex time-domain motion of such systems can easily be computed using the frequency-domain solution. We also extend the formulation to a focused incident wavepacket. The outline is as follows. In Section 2, we derive the equations of mo-

tion in the time and frequency domain. In Section 3, we show how the solution can be found using eigenfunction matching in the frequency domain. In Section 4, we illustrate how the solution in the time domain can be found straightforwardly from the frequency domain solutions.

We acknowledge that much of the material presented here has appeared in various previous works. In particular, the eigenfunction matching for a circular plate which underlies the calculations presented here. However, the present work aims to show how the time-domain solution can be found straightforwardly from the frequency domain solution. In some sense, the floating elastic plate is just a beautiful example to illustrate this method. We have given sufficient details of the solution method to understand the code that accompanies the paper. We also note that the code which accompanies this work is an essential part of it, and this has not been made available previously.

2. Equations of Motion

We consider here a floating elastic plate of uniform thickness and negligible draft. The plate is assumed to be circular with radius a. The fluid is of constant depth H with the z axis pointing vertically up and the free surface at $z = 0$. Such a plate has been the subject of extensive research. The displacement of the plate is denoted by w and the spatial velocity potential for the fluid by ϕ. The equation The plate has a uniform thickness h. This uniform thickness floating plate model has been the validated by laboratory experiments [45,46]. It reduces to that of a rigid body in the case of long waves.

We begin by stating the governing equations for the plate–water system, which was discussed in detail in [47], assuming that the equation of linear water waves governs the problem. The kinematic condition is

$$\partial_t w = \partial_z \Phi, \quad z = 0; \tag{1}$$

where w is the displacement of the fluid surface (which is also the plate displacement for $r < a$) and Φ is the velocity potential of the fluid. The dynamic condition is

$$\rho g w + \rho \partial_t \Phi = \begin{cases} \frac{E h^3}{12\,(1-\nu^2)} \partial_x^4 w + \rho_i h \partial_t^2 w, & r < a, \\ 0, & r > a \end{cases} \qquad z = 0; \tag{2}$$

where ρ is the water density, g is the gravitational acceleration, E is the Young's modulus of the plate, ν is its Poisson's ratio, and ρ_i is its density. Laplace's equation applies throughout the fluid

$$\Delta \Phi = 0, \ -H < z < 0 \tag{3}$$

and the usual non-flow condition at the bottom surface

$$\partial_z \Phi = 0, \ z = -H. \tag{4}$$

Assuming that all motions are time harmonic with radian frequency ω, the velocity potential of the water, Φ, can be expressed as

$$\Phi(\mathbf{x}, z, t) = \mathrm{Re}\left\{\phi(\mathbf{x}, z) \mathrm{e}^{-\mathrm{i}\omega t}\right\} \quad \text{and} \quad w(\mathbf{x}, t) = \mathrm{Re}\left\{\eta(\mathbf{x}) \mathrm{e}^{-\mathrm{i}\omega t}\right\}, \tag{5}$$

where the reduced velocity potential ϕ is complex-valued, and $\mathbf{x} = (x, y)$ is the horizontal spatial variable.

The frequency-domain potential satisfies the boundary value problem

$$\Delta \phi = 0, \quad -H < z < 0, \tag{6a}$$

$$\partial_z \phi = 0, \quad z = -H, \tag{6b}$$

$$\partial_z \phi = \alpha\, \phi, \quad z = 0, \, r > a, \tag{6c}$$

$$(\beta\bar{\Delta}^2 + 1 - \alpha\,\gamma)\partial_z\phi = \alpha\,\phi, \quad z = 0,\, r < a, \tag{6d}$$

where $\bar{\Delta}$ is the Laplacian operator in the horizontal plane. The constant $\alpha = \omega^2/g$ and β and γ are

$$\beta = \frac{E\,h^3}{12\,(1-\nu^2)\,\rho\,g} \quad \text{and} \quad \gamma = \frac{\rho_i\,h}{\rho}, \tag{7}$$

The free plate boundary conditions and the radiation condition need to be applied. Figure 1 gives a schematic diagram of the problem.

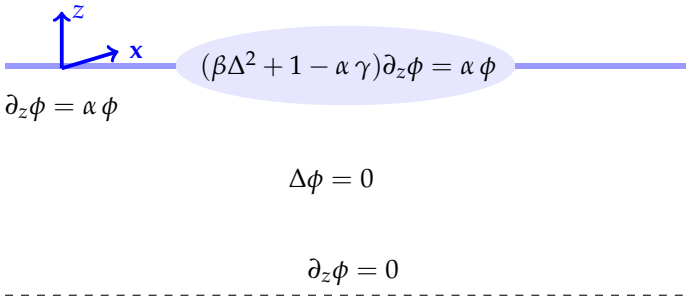

Figure 1. Frequency-domain equations for a floating circular plate.

3. Eigenfunction Matching

We derive the solution by the eigenfunction matching method here. The solution in two-dimensions first appeared in [7] and the three–dimensional solution was given in [9]. We begin by separating variables and writing

$$\phi(\mathbf{x}, z) = \zeta(z)X(\mathbf{x}). \tag{8}$$

Applying Laplace's equation, we obtain

$$\zeta_{zz} + \mu^2\zeta = 0, \tag{9}$$

so that

$$\zeta = \cos\mu(z + H), \tag{10}$$

where the separation constant μ^2 must satisfy the standard dispersion equations

$$k\tan(kH) = -\alpha, \quad \mathbf{x} \notin \Omega, \tag{11}$$

$$\kappa\tan(\kappa H) = \frac{-\alpha}{\beta\kappa^4 + 1 - \alpha\gamma}, \quad \mathbf{x} \in \Omega. \tag{12}$$

Note that we have set $\mu = k$ under the free surface and $\mu = \kappa$ under the plate. The dispersion equations are discussed in detail in [7]. We denote the negative imaginary solution of (11) by k_0 and the positive real by k_m, $m \geq 1$. The solutions of (12) are denoted by κ_m, $m \geq -2$. The fully complex with positive real part are κ_{-2} and κ_{-1} (where $\kappa_{-1} = \overline{\kappa_{-2}}$), the negative imaginary is κ_0 and the positive real are κ_m, $m \geq 1$. We define

$$\phi_m(z) = \frac{\cos k_m(z + H)}{\cos k_m H}, \quad m \geq 0, \tag{13}$$

as the vertical eigenfunction of the potential in the open water region and

$$\psi_m(z) = \frac{\cos \kappa_m(z + H)}{\cos \kappa_m H}, \quad m \geq -2, \tag{14}$$

as the vertical eigenfunction of the potential in the plate covered region.

We now use circular symmetry to write

$$X(\mathbf{x}) = \rho_n(r)\mathrm{e}^{\mathrm{i}n\theta} \tag{15}$$

where (r, θ) are the polar coordinates in the $\mathbf{x}$ direction. We now solve for the function $\rho_n(r)$. Using Laplace's equation in polar coordinates, we obtain

$$\frac{\mathrm{d}^2\rho_n}{\mathrm{d}r^2} + \frac{1}{r}\frac{\mathrm{d}\rho_n}{\mathrm{d}r} - \left(\frac{n^2}{r^2} + \mu^2\right)\rho_n = 0, \tag{16}$$

where μ is k_m or κ_m, depending on whether r is greater or less than a. We can convert this equation to the standard form by substituting $y = \mu r$ to obtain

$$y^2\frac{\mathrm{d}^2\rho_n}{\mathrm{d}y^2} + y\frac{\mathrm{d}\rho_n}{\mathrm{d}y} - (n^2 + y^2)\rho_n = 0. \tag{17}$$

The solution of this equation is a linear combination of the modified Bessel functions of order n, $I_n(y)$ and $K_n(y)$. Since the solution must be bounded, we know that under the plate it will be a linear combination of $I_n(y)$ while outside the plate will be a linear combination of $K_n(y)$. Therefore, the potential can be expanded as

$$\phi(r, \theta, z) = \sum_{n=-\infty}^{\infty}\sum_{m=0}^{\infty} a_{mn}K_n(k_m r)\mathrm{e}^{\mathrm{i}n\theta}\phi_m(z), \quad r > a, \tag{18}$$

$$\phi(r, \theta, z) = \sum_{n=-\infty}^{\infty}\sum_{m=-2}^{\infty} b_{mn}I_n(\kappa_m r)\mathrm{e}^{\mathrm{i}n\theta}\psi_m(z), \quad r < a, \tag{19}$$

where a_{mn} and b_{mn} are the coefficients in the open water and the plate covered region, respectively.

The incident potential is a wave of amplitude A in displacement travelling in the positive x-direction. Following [8], it can be written as

$$\phi^{\mathrm{I}} = \frac{A}{\mathrm{i}\sqrt{\alpha}}e^{k_0 x}\phi_0(z) = \sum_{n=-\infty}^{\infty} e_n I_n(k_0 r)\phi_0(z)\mathrm{e}^{\mathrm{i}n\theta} \tag{20}$$

where $e_n = A/\left(\mathrm{i}\sqrt{\alpha}\right)$.

The boundary conditions for the plate also have to be considered. The vertical force and bending moment must vanish, which can be written as

$$\left[\bar{\Delta} - \frac{1-\nu}{r}\left(\frac{\partial}{\partial r} + \frac{1}{r}\frac{\partial^2}{\partial\theta^2}\right)\right]\eta = 0, \tag{21}$$

and

$$\left[\frac{\partial}{\partial r}\bar{\Delta} - \frac{1-\nu}{r^2}\left(\frac{\partial}{\partial r} + \frac{1}{r}\right)\frac{\partial^2}{\partial\theta^2}\right]\eta = 0, \tag{22}$$

where w is the time-independent surface displacement, ν is Poisson's ratio, and $\bar{\Delta}$ is the in polar coordinates is

$$\bar{\Delta} = \frac{\partial^2}{\partial r^2} + \frac{1}{r}\frac{\partial}{\partial r} + \frac{1}{r^2}\frac{\partial^2}{\partial\theta^2} \tag{23}$$

The surface displacement and the velocity potential at the water surface are linked through the kinematic boundary condition

$$\phi_z = -\mathrm{i}\sqrt{\alpha}\eta \quad , z = 0 \tag{24}$$

The relationship between the potential and the surface displacement is

$$\eta = \mathrm{i}\sqrt{\alpha}\phi, \quad r > a \tag{25}$$

$$(\beta\bar{\Delta}^2 + 1 - \alpha\gamma)\eta = \mathrm{i}\sqrt{\alpha}\phi, \quad r < a. \tag{26}$$

The surface displacement can also be expanded in eigenfunctions as

$$\eta(r,\theta) = \sum_{n=-\infty}^{\infty}\sum_{m=0}^{\infty} \mathrm{i}\sqrt{\alpha}a_{mn}K_n(k_m r)\mathrm{e}^{\mathrm{i}n\theta}, \quad r > a, \tag{27}$$

$$\eta(r,\theta) = \sum_{n=-\infty}^{\infty}\sum_{m=-2}^{\infty} \mathrm{i}\sqrt{\alpha}(\beta\kappa_m^4 + 1 - \alpha\gamma)^{-1}b_{mn}I_n(\kappa_m r)\mathrm{e}^{\mathrm{i}n\theta}, \quad r < a,$$

using the fact that

$$\bar{\Delta}\left(I_n(\kappa_m r)\mathrm{e}^{\mathrm{i}n\theta}\right) = \kappa_m^2 I_n(\kappa_m r)\mathrm{e}^{\mathrm{i}n\theta}. \tag{28}$$

The boundary conditions (21) and (22) can be expressed in terms of the potential using (28). Since the angular modes are uncoupled, the conditions apply to each, giving

$$\sum_{m=-2}^{\infty}(\beta\kappa_m^4 + 1 - \alpha\gamma)^{-1}b_{mn}\times \left(\kappa_m^2 I_n(\kappa_m a) - \frac{1-\nu}{a}\left(\kappa_m I_n'(\kappa_m a) - \frac{n^2}{a}I_n(\kappa_m a)\right)\right) = 0, \tag{29}$$

and

$$\sum_{m=-2}^{\infty}(\beta\kappa_m^4 + 1 - \alpha\gamma)^{-1}b_{mn}\times \left(\kappa_m^3 I_n'(\kappa_m a) + n^2\frac{1-\nu}{a^2}\left(\kappa_m I_n'(\kappa_m a) + \frac{1}{a}I_n(\kappa_m a)\right)\right) = 0. \tag{30}$$

The potential and its derivative must be continuous across the transition from open water to the plate-covered region. Therefore, at $r = a$ they have to be equal. Again we know that this must be true for each angle and we obtain

$$e_n I_n(k_0 a)\phi_0(z) + \sum_{m=0}^{\infty} a_{mn}K_n(k_m a)\phi_m(z) = \sum_{m=-2}^{\infty} b_{mn}I_n(\kappa_m a)\psi_m(z), \tag{31}$$

and

$$e_n k_0 I_n'(k_0 a)\phi_0(z) + \sum_{m=0}^{\infty} a_{mn}k_m K_n'(k_m a)\phi_m(z) = \sum_{m=-2}^{\infty} b_{mn}\kappa_m I_n'(\kappa_m a)\psi_m(z), \tag{32}$$

for each n. We solve these equations by multiplying both by $\phi_l(z)$ and integrating from $-H$ to 0 to obtain

$$e_n I_n(k_0 a)A_0\delta_{0l} + a_{ln}K_n(k_l a)A_l = \sum_{m=-2}^{\infty} b_{mn}I_n(\kappa_m a)B_{ml} \tag{33}$$

$$e_n k_0 I_n'(k_0 a) A_0 \delta_{0l} + a_{ln} k_l K_n'(k_l a) A_l = \sum_{m=-2}^{\infty} b_{mn} \kappa_m I_n'(\kappa_m a) B_{ml}, \tag{34}$$

where

$$\int_{-H}^{0} \phi_m(z) \phi_n(z)\, \mathrm{d}z = A_m \delta_{mn}, \tag{35}$$

where

$$A_m = \frac{1}{2}\left(\frac{\cos k_m H \sin k_m H + k_m H}{k_m \cos^2 k_m H} \right), \tag{36}$$

and

$$\int_{-H}^{0} \phi_n(z) \psi_m(z)\, \mathrm{d}z = B_{mn}, \tag{37}$$

where

$$B_{mn} = \frac{k_n \sin k_n H \cos \kappa_m H - \kappa_m \cos k_n H \sin \kappa_m H}{(\cos k_n H \cos \kappa_m H)(k_n^2 - \kappa_m^2).} \tag{38}$$

Equation (33) can be solved for the open water coefficients a_{mn}

$$a_{ln} = -e_n \frac{I_n(k_0 a)}{K_n(k_0 a)} \delta_{0l} + \sum_{m=-2}^{\infty} b_{mn} \frac{I_n(\kappa_m a) B_{ml}}{K_n(k_l a) A_l}, \tag{39}$$

which can then be substituted into Equation (34) to give us

$$\left(k_0 I_n'(k_0 a) - k_0 \frac{K_n'(k_0 a)}{K_n(k_0 a)} I_n(k_0 a) \right) e_n A_0 \delta_{0l} = \sum_{m=-2}^{\infty} \left(\kappa_m I_n'(\kappa_m a) - k_l \frac{K_n'(k_l a)}{K_n(k_l a)} I_n(\kappa_m a) \right) B_{ml} b_{mn}, \tag{40}$$

for each n. Together with (29) and (30), (40) gives the required equations to solve for the coefficients of the water velocity potential in the plate covered region. For the numerical solution, we truncate the sum at N, and then we have $N+1$ equations from matching through the depth and two extra equations from the boundary conditions.

It should be noted that the solutions for positive and negative n are complex conjugates so that they do not both need to be calculated. There are some minor simplifications which are a consequence of this and are discussed in more detail in [8].

4. Time-Dependent Forcing and Numerical Results

We have denoted the surface displacement in the frequency domain is given by $\eta(\mathbf{x})$. However, the surface displacement is a function of ω and ω is a function of wavenumber k. We have also only considered waves incident from the positive x direction ($\theta = 0$). This choice of direction makes sense given the circular symmetry, but we can consider waves incident from other angles (found by rotation of the solution by the angle). Therefore, we denote the complex frequency domain surface displacement by $\eta((x), \theta, k)$.

4.1. Plane Incident Wave Forcing

The simplest time-dependent problem is to consider a place incident wave from the positive x direction. We assume that the incident wave is a Gaussian at $t = 0$. Therefore, the time–dependent displacement is then given by the following Fourier integral

$$w(\mathbf{x}, t) = \mathrm{Re}\left\{ \int_0^{\infty} \hat{f}(k) \eta(\mathbf{x}, 0, k) \mathrm{e}^{\mathrm{i}\omega t}\, \mathrm{d}k \right\}, \tag{41}$$

where $\hat{f}(k)$ is

$$\hat{f}(k) = \sqrt{\frac{\sigma}{\pi}} \exp(\sigma(k - k_0)^2). \tag{42}$$

where σ is a scale factor and we set $\sigma - 0.1$ and k_0 is the central wavenumber, we set $k_0 = 3$.

4.2. Focused Wave Group

It is more interesting to consider two-dimensional incident waves. A simple focused wave group can be constructed as from the following formula

$$w(\mathbf{x}, t) = \mathrm{Re}\left\{ \int_{-\pi/2}^{\pi/2} \int_0^{\infty} \hat{f}(k) \mathrm{e}^{-\theta_\sigma k^2 \sin^2(\theta)} \eta(\mathbf{x}, \theta, k) \mathrm{e}^{\mathrm{i}\omega t} \, \mathrm{d}k \, \mathrm{d}\theta \right\}, \tag{43}$$

where θ_σ is another scaling parameters which we set to be $\theta_\sigma = 0.1$

The numerical results we present are a subset of the possible motions which are possible. We fix the mass $\gamma = 0$, the water depth $h = 1$ and the floe radius $a = 2$ for all calculations. The solution is shown as an animation in movies 1 to 8, which are given as Supplementary Material. Figures 2–5 show snapshots from movies 1 to 4, respectively, for the times $t = -5, 0, 5, 10$. We change the stiffness from $\beta = 1 \times 10^{-1}$ in Figure 2 to $\beta = 1 \times 10^{-4}$ in Figure 5. The plate goes from being virtually stiff to highly flexible. The complex motion of the plate and fluid systems can be seen, especially in the movies in the Supplementary Material.

Figures 6–9 show the solution for the more complicated and interesting case of an incident wave packet. The complex and resonant behaviour of the plate and fluid system is clearly visible. In particular, the transition from the wave diffracting around the plate to the wave travelling under the plate as the stiffness transitions from high to low is visible. Moreover, we have an intermediate region where resonances exist, and the plate motion becomes highly complicated. The ability to visualise this motion offers insights which are not so easily obtained from the frequency domain solution.

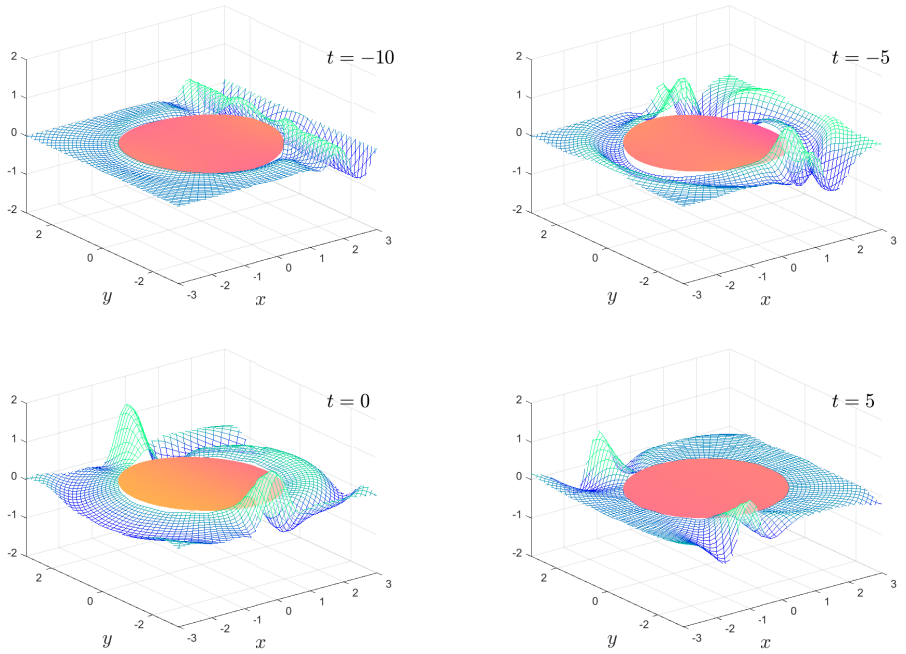

Figure 2. The time-dependent motion $\beta = 1 \times 10^{-1}$, $\gamma = 0$, $h = 1$ and $a = 2$ for the times shown. The full animation can be found in movie 1.

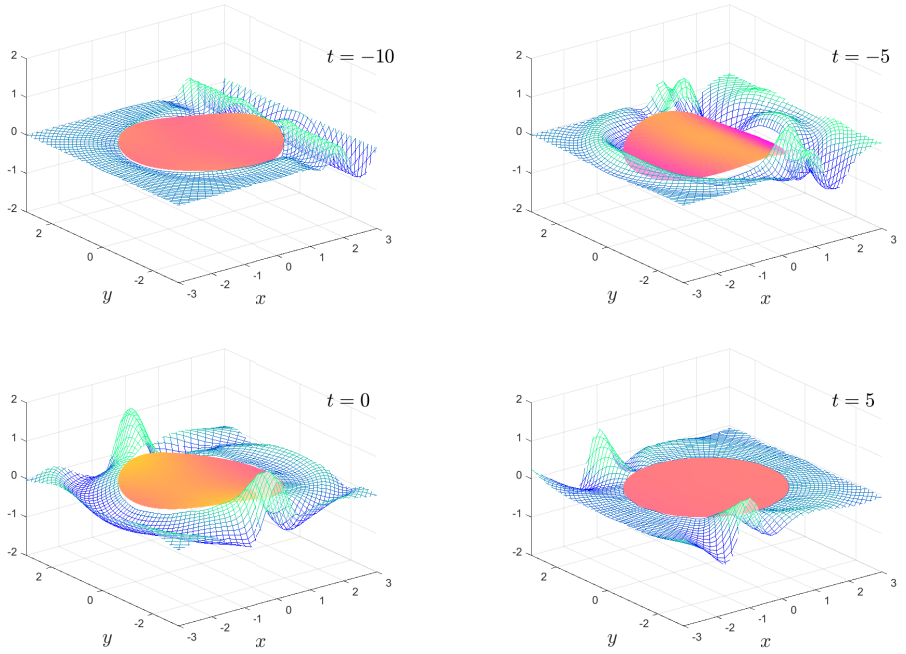

Figure 3. As in Figure 2, except $\beta = 1 \times 10^{-2}$. The full animation can be found in movie 2.

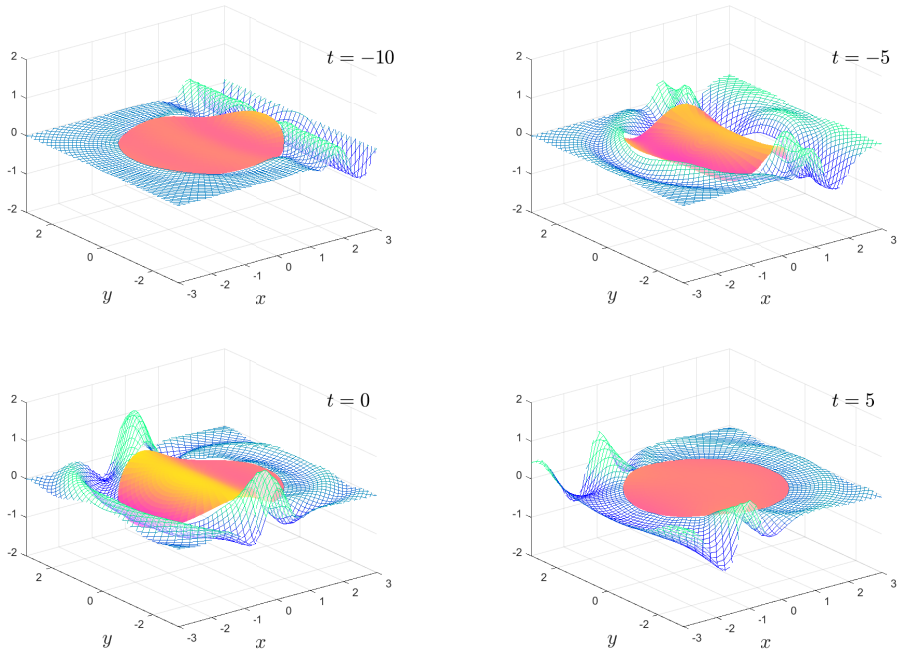

Figure 4. As in Figure 2, except $\beta = 1 \times 10^{-3}$. The full animation can be found in movie 3.

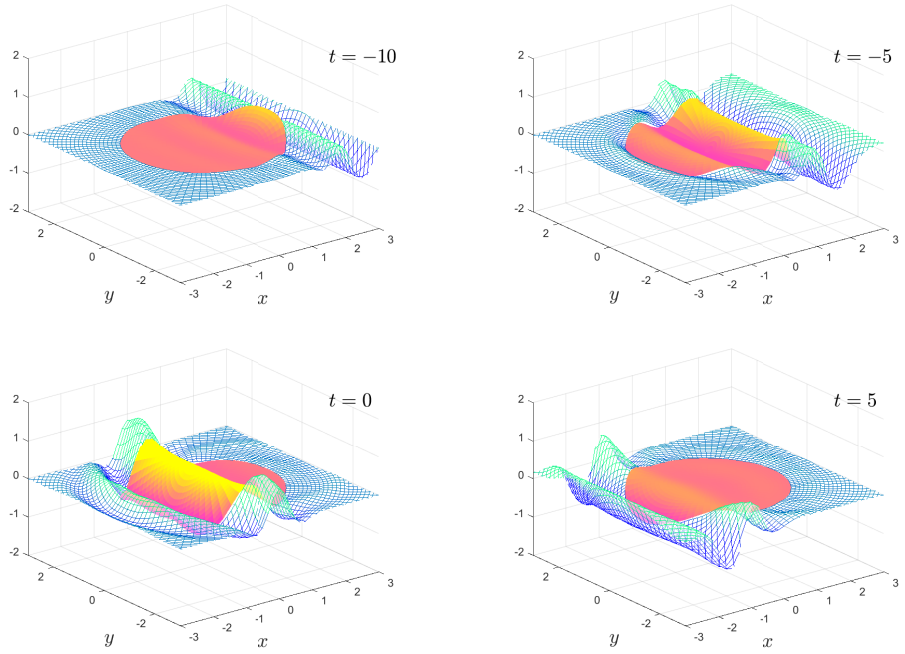

Figure 5. As in Figure 2, except $\beta = 1 \times 10^{-4}$. The full animation can be found in movie 4.

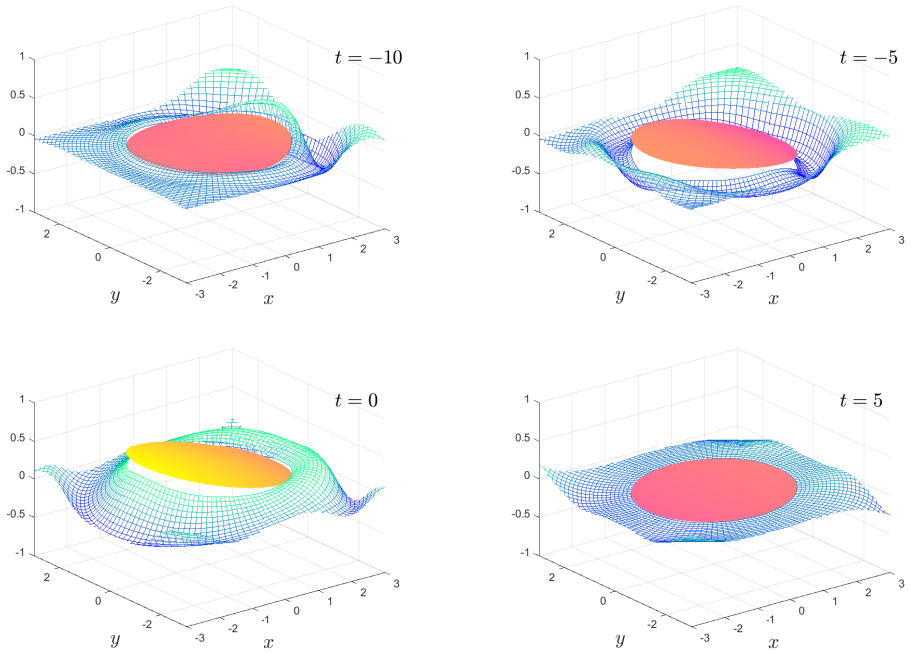

Figure 6. The time-dependent motion $\beta = 1 \times 10^{-1}$, $\gamma = 0$, $h = 1$ and $a = 2$ for the times shown. The full animation can be found in movie 5.

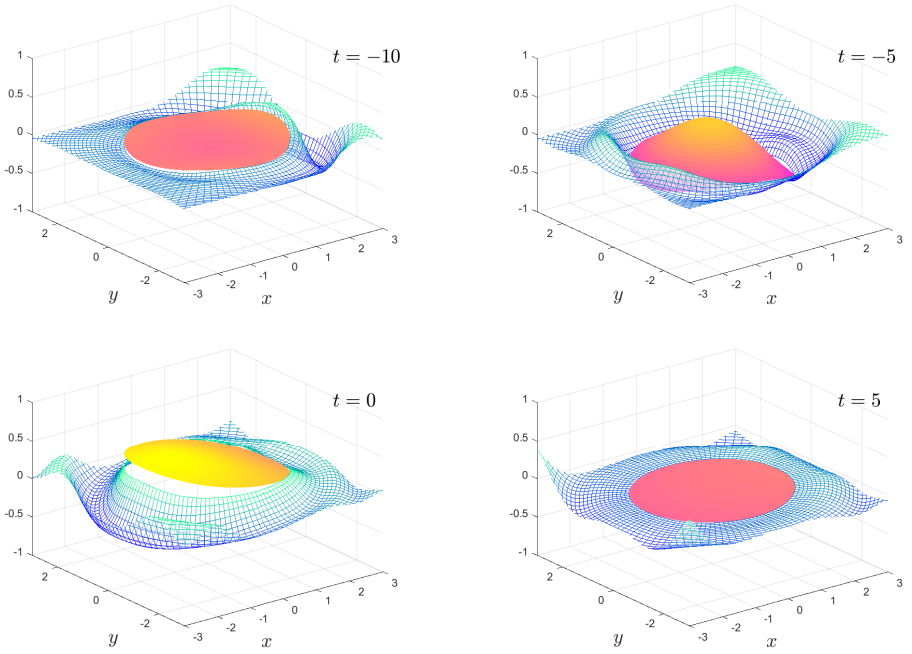

Figure 7. As in Figure 6, except $\beta = 1 \times 10^{-3}$. The full animation can be found in movie 6.

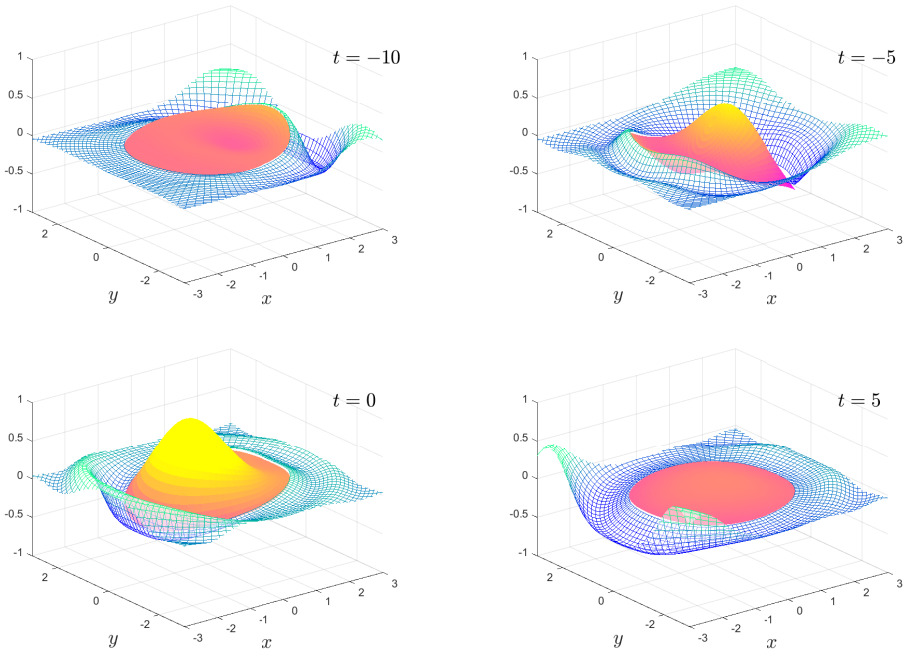

Figure 8. As in Figure 6, except $\beta = 1 \times 10^{-4}$. The full animation can be found in movie 7.

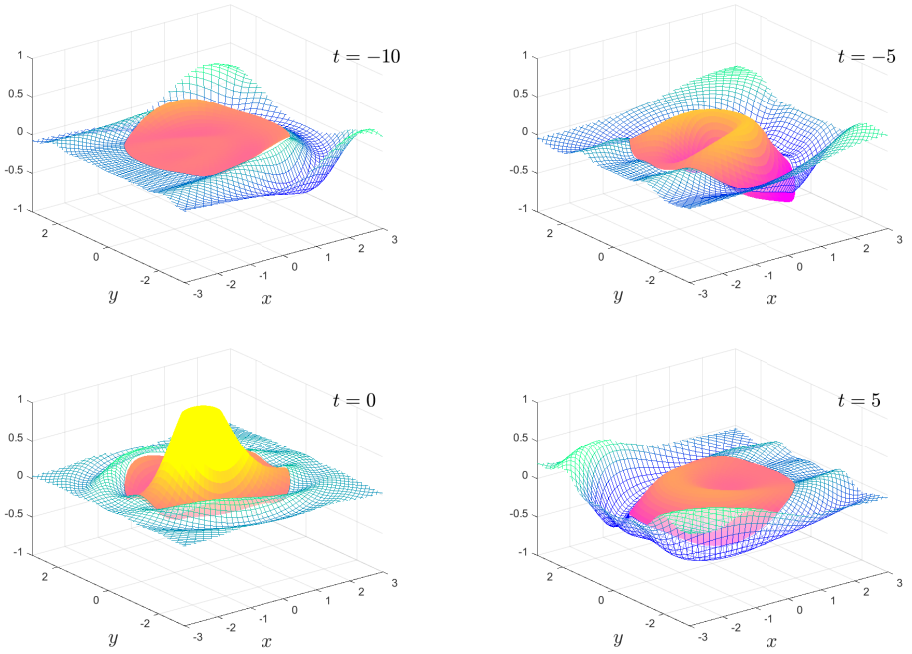

Figure 9. As in Figure 6, except $\beta = 1 \times 10^{-2}$. The full animation can be found in movie 8.

5. Conclusions

The purpose of this work is to show how we can easily visualise the complex time-domain behaviour of complex wave scattering problems such as those which arise from the scattering by a flexible plate. While the frequency–domain solution is central to our calculations, the scattering results from the frequency domain solution are often challenging to interpret in the context of incident wave packets. By the simple visualisation using the suitable superposition of incident waves, we can bring the complex motion to life. The author hopes that these results, and the accompanying computer code, will encourage others to also investigate such visualisations for their complex water wave scattering problem.

Supplementary Materials: The following are available at https://www.mdpi.com/2311-5521/6/1/29/s1, The movie files and MATLAB code are provided as Supplementary Material.

Funding: This work is funded by the Australian Research Council (DP200102828).

Data Availability Statement: The MATLAB code to make the calculations is provided as Supplementary Material.

Conflicts of Interest: The author declares no conflict of interest.

References

1. Bishop, R.E.D.; Price, W.G.; Wu, Y. A General Linear Hydroelasticity Theory of Floating Structures Moving in a Seaway. *Philos. Trans. R. Soc.* **1986**, *316*, 375–426.
2. Kashiwagi, M. Research on Hydroelastic Response of VLFS: Recent Progressand Future Work. *Int. J. Offshore Polar Eng.* **2000**, *10*, 81–90.
3. Squire, V.A. Synergies Between VLFS Hydroelasticity and Sea Ice Research. *Int. J. Offshore Polar Eng.* **2008**, *18*, 1–13.
4. Watanabe, E.; Utsunomiya, T.; Wang, C.M. Hydroelastic analysis of pontoon-type VLFS: A literature survey. *Eng. Struct.* **2004**, *26*, 245–256. [CrossRef]
5. Newman, J.N. Wave effects on deformable bodies. *Appl. Ocean Res.* **1994**, *16*, 45–101. [CrossRef]
6. Meylan, M.H.; Squire, V.A. The Response of Ice Floes to Ocean Waves. *J. Geophy. Res.* **1994**, *99*, 891–900. [CrossRef]
7. Fox, C.; Squire, V.A. On the Oblique Reflexion and Transmission of Ocean Waves at Shore Fast Sea Ice. *Philos. Trans. R. Soc. Lond. A* **1994**, *347*, 185–218.
8. Zilman, G.; Miloh, T. Hydroelastic Buoyant Circular Plate in Shallow Water: A Closed Form Solution. *Appl. Ocean Res.* **2000**, *22*, 191–198. [CrossRef]

9. Peter, M.A.; Meylan, M.H.; Chung, H. Wave scattering by a circular elastic plate in water of finite depth: A closed form solution. *Int. J. Offshore Polar Eng.* **2004**, *14*, 81–85.
10. Bennetts, L.G.; Biggs, N.R.T.; Porter, D. A multi-mode approximation to wave scattering by ice sheets of varying thickness. *J. Fluid Mech.* **2007**, *579*, 413–443. [CrossRef]
11. Balmforth, N.; Craster, R. Ocean waves and ice sheets. *J. Fluid Mech.* **1999**, *395*, 89–124.
12. Chung, H.; Fox, C. Calculation of wave-ice interaction using the Wiener-Hopf technique. *N. Z. J. Math.* **2002**, *31*, 1–18.
13. Davys, J.W.; Hosking, R.J.; Sneyd, A.D. Waves due to a Steadily Moving Source on a Floating Ice Plate. *J. Fluid Mech.* **1985**, *158*, 269–287. [CrossRef]
14. Hosking, R.J.; Sneyd, A.D.; Waugh, D.W. Viscoelastic Response of a Floating Ice Plate to a Steadily Moving Load. *J. Fluid Mech.* **1988**, *196*, 409–430. [CrossRef]
15. Milinazzo, F.; Shinbrot, M.; Evans, N.W. A Mathematical Analysis of the Steady Response of Floating Ice to the Uniform Motion of a Rectangular Load. *J. Fluid Mech.* **1995**, *287*, 173–197.
16. Squire, V.A.; Hosking, R.J.; Kerr, A.D.; Langhorne, P.J. *Moving Loads on Ice Plates*; Kluwer: Alphen aan den Rijn, The Netherlands, 1996.
17. Nugroho, W.; Wang, K.; Hosking, R.; Milinazzo, F. Time-dependent response of a floating flexible plate to an impulsively started steadily moving load. *J. Fluid Mech.* **1999**, *381*, 337–355.
18. Wang, K.; Hosking, R.; Milinazzo, F. Time-dependent response of a floating viscoelastic plate to an impulsively started moving load. *J. Fluid Mech.* **2004**, *521*, 295–317. [CrossRef]
19. Bonnefoy, F.; Meylan, M.; Ferrant, P. Nonlinear higher-order spectral solution for a two-dimensional moving load on ice. *J. Fluid Mech.* **2009**, *621*, 215–242.
20. Meylan, M.H. The forced vibration of a thin plate floating on an infinite liquid. *J. Sound Vib.* **1997**, *205*, 581–591.
21. Meylan, M.H. Spectral Solution of Time Dependent Shallow Water Hydroelasticity. *J. Fluid Mech.* **2002**, *454*, 387–402.
22. Sturova, I.V. Unsteady behavior of an elastic beam floating on shallow water under external loading. *J. Appl. Mech. Tech. Phys.* **2002**, *43*, 415–423. [CrossRef]
23. Sturova, I.V. The action of an unsteady external load on a circular elastic plate floating on shallow water. *J. Appl. Maths Mechs.* **2003**, *67*, 407–416. [CrossRef]
24. Meylan, M.H. The time-dependent vibration of forced floating elastic plates by eigenfunction matching in two and three dimensions. *Wave Motion* **2019**, *88*, 21–33. [CrossRef]
25. Tkacheva, L. Plane problem of vibrations of an elastic floating plate under periodic external loading. *J. Appl. Mech. Tech. Phys.* **2004**, *45*, 420–427. [CrossRef]
26. Tkacheva, L. Action of a periodic load on an elastic floating plate. *Fluid Dyn.* **2005**, *40*, 282–296. [CrossRef]
27. Hazard, C.; Meylan, M.H. Spectral theory for a two-dimensional elastic thin plate floating on water of finite depth. *SIAM J. Appl. Math.* **2007**, *68*, 629–647. [CrossRef]
28. Meylan, M.H.; Sturova, I.V. Time-Dependent Motion of a Two-Dimensional Floating Elastic Plate. *J. Fluid. Struct.* **2009**, *25*, 445–460.
29. Kashiwagi, M. A Time-Domain Mode-Expansion Method for Calculating Transient Elastic Responses of a Pontoon-Type VLFS. *J. Mar. Sci. Technol.* **2000**, *5*, 89–100. [CrossRef]
30. Kashiwagi, M. Transient responses of a VLFS during landing and take-off of an airplane. *J. Mar. Sci. Technol.* **2004**, *9*, 14–23. [CrossRef]
31. Qui, L. Numerical simulation of transient hydroelastic response of a floating beam induced by landing loads. *Appl. Ocean Res.* **2007**, *29*, 91–98.
32. Matiushina, A.A.; Pogorelova, A.V.; Kozin, V.M. Effect of Impact Load on the Ice Cover During the Landing of an Airplane. *Int. J. Offshore Polar Eng.* **2016**, *26*, 6–12. [CrossRef]
33. Endo, H.; Yago, K. Time history response of a large floating structure subjected to dynamic load. *J. Soc. Nav. Archit. Jpn.* **1999**, *1999*, 369–376. [CrossRef]
34. Montiel, F.; Bennetts, L.; Squire, V. The transient response of floating elastic plates to wavemaker forcing in two dimensions. *J. Fluids Struct.* **2012**, *28*, 416–433. [CrossRef]
35. Skene, D.; Bennetts, L.; Wright, M.; Meylan, M.; Maki, K. Water wave overwash of a step. *J. Fluid Mech* **2018**, *839*, 293–312. [CrossRef]
36. Huang, L.; Ren, K.; Li, M.; Tuković, Ž.; Cardiff, P.; Thomas, G. Fluid-structure interaction of a large ice sheet in waves. *Ocean Eng.* **2019**, *182*, 102–111. [CrossRef]
37. Nelli, F.; Bennetts, L.G.; Skene, D.M.; Toffoli, A. Water wave transmission and energy dissipation by a floating plate in the presence of overwash. *J. Fluid Mech.* **2020**, *889*, A19. [CrossRef]
38. Tran-Duc, T.; Meylan, M.H.; Thamwattana, N.; Lamichhane, B.P. Wave Interaction and Overwash with a Flexible Plate by Smoothed Particle Hydrodynamics. *Water* **2020**, *12*, 3354. [CrossRef]
39. Meylan, M.; Bennetts, L.; Cavaliere, C.; Alberello, A.; Toffoli, A. Experimental and theoretical models of wave-induced flexure of a sea ice floe. *Phys. Fluids* **2015**, *27*, 041704. [CrossRef]
40. Kohout, A.L.; Meylan, M.H. Wave Scattering by Multiple Floating Elastic Plates with Spring or Hinged Boundary Conditions. *Mar. Struct.* **2009**, *22*, 712–729. [CrossRef]

41. Kohout, A.L.; Meylan, M.H. An elastic plate model for wave attenuation and ice floe breaking in the marginal ice zone. *J. Geophys. Res.* **2008**, *113*. [CrossRef]
42. Kohout, A.L.; Meylan, M.H.; Sakai, S.; Hanai, K.; Leman, P.; Brossard, D. Linear Water Wave Propagation Through Multiple Floating Elastic Plates of Variable Properties. *J. Fluid. Struct.* **2007**, *23*, 649–663. [CrossRef]
43. Mahmood-ul-Hassan; Meylan, M.H.; Peter, M.A. Water-Wave Scattering by Submerged Elastic Plates. *Quart. J. Mech. Appl. Math.* **2009**, *62*, 321–344. [CrossRef]
44. Behera, H.; Sahoo, T. Hydroelastic analysis of gravity wave interaction with submerged horizontal flexible porous plate. *J. Fluids Struct.* **2015**, *54*, 643–660. [CrossRef]
45. Montiel, F.; Bennetts, L.G.; Squire, V.A.; Bonnefoy, F.; Ferrant, P. Hydroelastic response of floating elastic discs to regular waves. Part 1. Wave basin experiments. *J. Fluid Mech.* **2013**, *723*, 604–628. [CrossRef]
46. Montiel, F.; Bennetts, L.G.; Squire, V.A.; Bonnefoy, F.; Ferrant, P. Hydroelastic response of floating elastic discs to regular waves. Part 1. Modal analysis. *J. Fluid Mech.* **2013**, *723*, 629–652. [CrossRef]
47. Meylan, M.H. The Wave Response of Ice Floes of Arbitrary Geometry. *J. Geophys. Res.* **2002**, *107*. [CrossRef]